A reduced order model based on sector mistuning for the dynamicanalysis of mistuned bladed disks

A reduced order model based on sector mistuning for the dynamic analysis of mistuned bladed disks

P. Vargiu*, C.M. Firrone, S. Zucca, M.M. Gola

Department of Mechanics, Politecnico di Torino, C.so Duca degli Abruzzi 24, 10129, Torino, Italy

Abstract

In this paper, a pre-existing reduction technique suitable for the analysis of mistuned bladed disk dynamics, the Component Mode Mistuning technique (CMM), originally developed exclusively for the use of blade frequency mistuning pattern, is extended in order to allow for the introduction of a sector frequency mistuning pattern. If either mistuning is not confined to the blades (i.e. blades-to-disk interface mistuning), or the blades can not be removed from the bladed disk (i.e. integral bladed disks), sector mistuning rather than blade mistuning is a more suitable choice to perturb the tuned system. As a consequence, the extension of the original technique is referred as Integral Mode Mistuning (IMM). After a theory review of the original technique, the modifications leading to the IMM are described. Finally, the proposed IMM technique is validated in terms of both modal parameters estimation and forced response calculation, by means of a dummy bladed disk developed at Politecnico di Torino.

Keywords: Bladed disk dynamics, Mistuning, Order reduction technique

1. Introduction

. An industrial rotor generally is a very complex structure. Using a complete finite element model (FEM), in order to predict the dynamic behaviour and the stress outline of the bladed disk, is often a formidable task, due to the high computational cost needed by the calculation (an industrial FE model

*Phone: +390110906953
E-mail: paolo.vargiu@polito.it

easily consists of millions of nodes). Consequently, a model simplification is usually requested, without any loss of accuracy; this target is reached noting that a bladed disk can be subdivided in sectors, everyone ideally equal to each other. This property, called *cyclic symmetry*, allows to analyse the whole structure by using only the FE model of the fundamental sector, following for instance the approach proposed by Mead [2] and Thomas [3]. The dynamic behaviour of such structures is mainly characterized by the presence of double natural frequencies, corresponding to twin mode shapes counter-rotating along the system. Although a bladed disk is generally designed in order to reproduce the perfect cyclic symmetry conditions, the real rotors are always characterized by random deviations among the sectors, caused by manufacturing tolerances, material defectiveness, non-uniform assembly or wear. This issue is commonly called *mistuning*, which destroys the cyclic symmetry of the structure. The effects of the introduction of irregularities on a tuned structure have been extensively studied by the research community from the early 60's (Ewins [1]; Hodges [4], [5]; Kissel, [8]; Pierre, [9]): even though mistuning is typically small, it causes the split of the double natural frequencies, a distortion of the mode shapes and, above all, mistuned bladed disks can experience drastically larger forced response levels than the ideal, tuned design, as outlined by Whitehead in [13] and MacBain et al. in [7]. The unexpected increase in maximum stresses can lead to premature high cycle fatigue (HCF) of the blades. It is clearly of great interest to be able to predict the maximum blade response as a result of mistuning. The most used approach to analyse mistuning effects on bladed disks is a statistical method, through Monte Carlo simulations, in order to evaluate the maximum possible blade forced response, as highlighted in [20]. It is well known that the accuracy obtainable from Monte Carlo techniques improves as the number of iterations grows, especially in case of rare events. This commonly makes unusable the FEM of the whole structure, due to the tremendously high computational cost required for the analysis. From this considerations the development of purpose-made FEM reduction techniques is necessary, in order to obtain more compact, but also accurate, models.

Introducing the mistuning definition, we usually refer to the so-called *geometrical mistuning*, i.e. the physical perturbations occurring in the real structural parameters. Clearly, the introduction of a geometrical mistuning into the reduced-order models (ROMs) means that all the degrees of freedom (dofs) where mistuning is present must be retained. Moreover, especially when one wants to analyse a real, manufactured bladed disk through a

ROM, FEM or lumped mass model, there is usually no way to measure or determine the geometrical mistuning in the structure. An alternative mistuning model has to be considered: the *frequency mistuning*. In fact a geometrical mistuning, whatever its nature is, has the effect of modifying the structure natural frequencies with respect to the ideal tuned configuration. Furthermore, the frequency perturbation is a quantity directly measurable and easy to be introduced into the ROMs. Therefore, by swapping the cause with the effect, the geometrical mistuning (cause) is substituted into the ROMs by the frequency mistuning (effect). This is the approach mainly used in the literature, where two frequency mistuning models have been introduced: (i) the *blade frequency mistuning* model, used in the vast part of the ROMs, defined as the deviation of the single, cantilevered-blade mistuned natural frequencies from the corresponding tuned ones; (ii) the *sector frequency mistuning* model, firstly introduced by Griffin et al. in [18], where the natural frequency deviations are referred to the whole fundamental sector.

The choice of the blade mistuning as the most important (and, often, as the only important) mistuning model is due to the high sensitivity shown by the blade-dominated modes (high modal density regions) to the presence of irregularities. However, Griffin et al. pointed out that the blade mistuning is not the proper model to analyse the integrally manufactured bladed disks (*blisks*), due to the impossibility to physically separate the blades from the disk. Moreover, a perturbation in the disk-to-blade interface (for instance, the stagger angle of the blades) can not be captured by a blade frequency mistuning model. In order to fill this gap, they proposed an alternative mistuning model, which considers the frequency deviation of the whole sector. The importance of the blade-to-disk interface mistuning has been recently confirmed by Mignolet et al. in [22]: considering the FE model of a non-integral bladed disk, they showed how the highest forced response amplifications obtained with a mistuning pattern in the disk-to-blade interfaces can be compared to those occurring when only the blades are mistuned.

Several model reduction techniques have been proposed in literature in order to analyse the mistuned bladed disk dynamics: as mentioned, the vast part of them accounts only for a blade frequency mistuning model, like for instance REDUCE [11], SNM [15], MISTRES [17], CMM [21]; just FMM [16] allows to account also for a sector mistuning. However, the great simplifications introduced in this high-reduced model lead to a limitation of its applicability, i.e. only to isolated and blade-dominated families of modes. This restriction prevents, for instance, from the analysis of the so-called

veering regions, also characterized by high sensitivity to mistuning effects, as mentioned in [20].

The aim of the work described in this paper is the development of a ROM which takes into account a sector frequency mistuning model without introducing any restriction for its application. For this purpose, one of the higher-performing models, CMM, has been selected to provide an extended technique, referred as IMM. Firstly, the original CMM theory is briefly resumed. Then, the proposed IMM model is described in details. Finally, the IMM model is validated through the model reduction of a realistic dummy bladed disk, where two types of mistuning are applied: a disk-to-blade interfaces mistuning, and a blade elastic modulus mistuning; the validation process serves also to highlight as the introduction of the blade frequency mistuning model only does not always guarantee a correct modelling of the whole bladed disk dynamics.

2. CMM (Component Mode Mistuning) theory

. The CMM reduction technique was proposed by Lim et al. in [21]. This model can be classified as C.M.S. technique, and in particular belongs to the hybrid-interface component class. Let us consider the classical equation of motion of a cyclic mistuned system:

$$\left(-\omega^2 \cdot M + i\omega \cdot C + K\right) \cdot \{x_0\} = \{F\} \tag{1}$$

where the vector $\{F\}$ is the rotating force acting on the structure. The force system acting on the complete structure may be called a rotating force system if the force acting on any degree of freedom of one sector $n-1$ has the same amplitude as the force acting on the same degree of freedom in the nth following sector, and there is a fixed phase difference between them (depending on the force periodicity):

$$\{F\}_n \cdot e^{i\omega t} = \{F\}_{n-1} \cdot e^{i(\omega t - EO\phi)} = F_0 \cdot e^{i(\omega t - (n-1)EO\phi)}; \tag{2}$$

where EO is the Engine Order of the excitation, $\phi = 2\pi/N$ is the sector geometric angle, $n = 1, \cdots, N$ is the number of blades and F_0 is the amplitude of the force.

The key-idea of this technique is to substructure the mistuned bladed disk in two components: the first substructure is the whole tuned bladed disk, the second corresponds to the perturbation produced by mistuning on the blades only, as shown in Figure 1(a). As a consequence, the interfaces between the components previously defined consist of *all the blade degrees of freedom*; the model reduction of each component is here described:

1. **Tuned bladed disk**, treated as free-interface component, whose mass-normalized normal modes $[\phi^s]$ are a restricted set of the whole structure tuned modes. In order to guarantee the correct static behaviour of the structure, a set of attachment modes $[\psi^s]$ are needed; these static deflections are computed by imposing, one-by-one, a unity force to a single interface dof while keeping the other dofs unloaded. By applying a coordinate transformation through the transformation matrix $\left[\begin{array}{cc} \phi^s & \psi^s \end{array}\right]$, the equation of motion of the component becomes:

$$\left(-\omega^2 \cdot \mu^s + i\omega \cdot c^s + \kappa^s\right) \cdot \{p^s\} = \left[\begin{array}{cc} \phi^s & \psi^s \end{array}\right]^T \cdot \{F\}\,; \tag{3}$$

where:

$$\mu^s = \left[\begin{array}{cc} \phi^s & \psi^s \end{array}\right]^T \cdot [M^s] \cdot \left[\begin{array}{cc} \phi^s & \psi^s \end{array}\right] = \\ = \left[\begin{array}{cc} I & \phi^{sT} \cdot M^s \cdot \psi^s \\ \psi^{sT} \cdot M^s \cdot \phi^s & \psi^{sT} \cdot M^s \cdot \psi^s \end{array}\right]; \tag{4}$$

$$\kappa^s = \left[\begin{array}{cc} \phi^s & \psi^s \end{array}\right]^T \cdot [K^s] \cdot \left[\begin{array}{cc} \phi^s & \psi^s \end{array}\right] = \\ = \left[\begin{array}{cc} \Lambda^s & \phi^{sT} \cdot K^s \cdot \psi^s \\ \psi^{sT} \cdot K^s \cdot \phi^s & \psi^{sT} \cdot K^s \cdot \psi^s \end{array}\right]; \tag{5}$$

$$c^s = diag\left(2\zeta\omega_i\right); \tag{6}$$

are, respectively, the modal mass, stiffness and damping matrices, the vector $\{p^s\} = \left\{\begin{array}{cc} p^s & p^s_\psi \end{array}\right\}^T$ contains the generalized coordinates and the submatrix Λ^s includes the tuned eigenvalues in the main diagonal. Note that the tuned matrices $[M^s]$ and $[K^s]$ are block circulant.

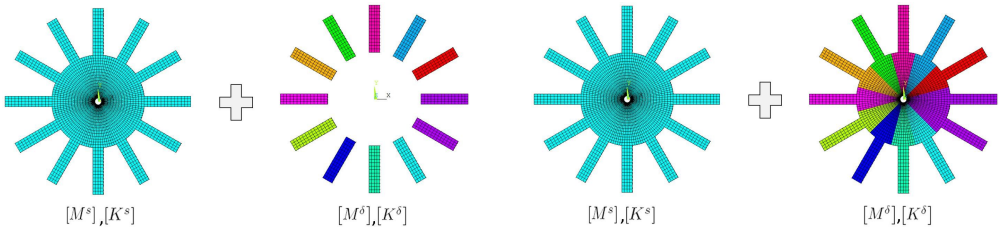

(a) CMM. (b) IMM.

Figure 1: Bladed disk substructuring.

2. **Blade mistuning component**, consisting of all the blades which structural matrices, $\left[M^\delta\right]$ and $\left[K^\delta\right]$, contain only the perturbations of the tuned ones. This component is treated as fixed-interface component, so a set of constraint modes $\left[\psi^\delta\right]$ is necessary to complete the model. Consequently, for this second component no normal modes are available, since all the blade dofs are fixed, and constraint modes $\left[\psi^\delta\right]$ only are used. In this case, these static deflections are computed by imposing, one-by-one, a unity displacement to a single interface dof while keeping the other dofs fixed. Therefore, such constraint modes matrix is equal to the identity matrix $[I]$. The final mass and stiffness modal matrices of the component are equal to the unreduced $\left[M^\delta\right]$ and $\left[K^\delta\right]$:

$$\mu^\delta = [I]^T \cdot \left[M^\delta\right] \cdot [I] = \left[M^\delta\right] \ , \ \kappa^\delta = [I]^T \cdot \left[K^\delta\right] \cdot [I] = \left[K^\delta\right] . \qquad (7)$$

Note that the matrices $\left[M^\delta\right]$ and $\left[K^\delta\right]$ are block diagonal since the blades are not directly coupled among themselves.

As stated before, the component-to-component interfaces consist of all the blade dofs. Consequently, the number of static deformed shapes $[\psi^s]$ and $\left[\psi^\delta\right]$ necessary for the two reduced components is equal to the number of blades dofs.

The assembly between the mass and stiffness matrices of the components is performed by imposing the congruence of the displacements at the mating interfaces, i.e. $\{x_b^s\} = \left\{x^\delta\right\}$; subscript b, hereinafter, indicates a vector or matrix containing quantities related to the blade dofs only. The final equation of motion of the whole system is:

$$\left(-\omega^2 \cdot \mu^{rom} + i\omega \cdot c^{rom} + \kappa^{rom}\right) \cdot \{p^{rom}\} = \left[\begin{array}{cc} \phi^s & \psi^s \end{array} \right]^T \cdot \{F\} \,. \tag{8}$$

where the model structural matrices are:

$$\mu^{rom} = \mu^s + \left[\begin{array}{cc} \phi_b^{sT} \cdot M^\delta \cdot \phi_b^s & \phi_b^{sT} \cdot M^\delta \cdot \psi_b^s \\ \psi_b^{sT} \cdot M^\delta \cdot \phi_b^s & \psi_b^{sT} \cdot M^\delta \cdot \psi_b^s \end{array} \right]; \tag{9}$$

$$\kappa^{rom} = \kappa^s + \left[\begin{array}{cc} \phi_b^{sT} \cdot K^\delta \cdot \phi_b^s & \phi_b^{sT} \cdot K^\delta \cdot \psi_b^s \\ \psi_b^{sT} \cdot K^\delta \cdot \phi_b^s & \psi_b^{sT} \cdot K^\delta \cdot \psi_b^s \end{array} \right]; \tag{10}$$

Due to the presence of the attachment modes $[\psi^s]$, the employment of such technique is quite expensive from a computational point of view. However, in the case of small mistuning, some approximations can be introduced in order to reduce the model dimension.

2.1. Small mistuning approximations

. Following the concept developed by Griffin et al. in [12], dealing with the restricted number of tuned modes needed to obtain the mistuned ones by linear combination, Lim et al. proposed to neglect the attachment modes $[\psi^s]$, since they do not contribute to the mistuned modes generation in the high modal density region. The simplified matrices of the CMM model so are:

$$[\mu_{sm}^{rom}] = [I] + \left[\phi_b^{sT} \cdot M^\delta \cdot \phi_b^s\right] \;,\; [\kappa_{sm}^{rom}] = [\Lambda^s] + \left[\phi_b^{sT} \cdot K^\delta \cdot \phi_b^s\right], \tag{11}$$

where subscript *sm* refers to the small mistuning hypothesis.

After the approximation mentioned about, the model dimension is reduced to the number of tuned modes retained into the analysis. However, the computation of $[\mu_{sm}^{rom}]$ and $[\kappa_{sm}^{rom}]$ still requires a high computational cost, since they involve products among matrices whose dimensions are equal to the number of all the N blades dofs. Furthermore, a frequency mistuning model can not be introduced yet.

In order to overcome this problem, the authors used an approach proposed by Bladh et al. in [14], the *mistuning projection method*, according to which

the mistuned matrices are reduced through the projection over the unperturbed mode shapes. Let us consider a single, mistuned cantilevered blade, whose mistuned stiffness matrix and tuned modal matrix are, respectively, $[K_b^{mist}]$ and $[\phi_b^0]$; then, defined the matrix product:

$$\left[\kappa^{mist}\right] = \left[\phi_b^0\right]^T \cdot \left[K_b^{mist}\right] \cdot \left[\phi_b^0\right], \tag{12}$$

the mistuning projection method, in absence of mass mistuning, allows to approximate the diagonal terms of the matrix above as:

$$\kappa_{pp}^{mist} = \delta_b \cdot \lambda_{b,p}^0 \qquad \text{with} \qquad p = 1, \cdots P, \tag{13}$$

where δ_b is the blade frequency deviation in respect to the pth unperturbed cantilevered blade eigenvalue $\lambda_{b,p}^0$, and P is a restricted set of eigenvectors $[\phi_b^0]$. Note that the matrix $[\kappa^{mist}]$ is diagonal if the mistuning is proportional to the global stiffness matrix $[K_b^{mist}]$, since the blade mistuned mode shapes are not generally distorted; however, in case of slightly distorted blade mode shapes, the diagonal terms are predominant in respect of the off-diagonal ones, so the (13) still holds.

In order to apply the mistuning projection method to the CMM formulation, the unperturbed cantilevered blade modes must be expressed in the (11). This is achieved by computing the modal partecipation factors of the cantilevered blade modes $[\phi_b^0]$ in the blade portions of the tuned modes $[\phi_b^s]$:

$$[\phi_b^s] = \left[\phi_b^0\right] \cdot [q]. \tag{14}$$

Using the cyclic symmetry properties, the participation factors $[q]$ are obtainable from the tuned mode shapes referred to the single blade, through the relation:

$$\left[\phi_b^0\right]^T \cdot \left[K_b^0\right] \cdot \left[\tilde{\phi}_b^{s,h}\right] = \left[\phi_b^0\right]^T \cdot \left[K_b^0\right] \cdot \left[\phi_b^0\right] \cdot \left[\tilde{q}^h\right]_n = \left[\Lambda_b^0\right] \cdot \left[\tilde{q}^h\right]_n; \tag{15}$$

where $[\tilde{q}]$ are the modal participation factors expressed in a cyclic symmetry fashion, the superscript h denotes the harmonic number of the tuned eigenvector considered and the subscript n indicates the blade number, with

$n = 1, \cdots, N$. The modal participation vector $[q]$ of the whole structure is finally obtainable through the cyclic expansion:

$$[q] = (\mathcal{F} \otimes I) \cdot \underset{h=0\ldots N/2}{Bdiag} \left[\tilde{q}^h\right]; \tag{16}$$

where $\otimes$ indicates the Kronecker product and $\mathcal{F}$ is a real-valued form of the Fourier matrix, as defined in [11]. The final form of the CMM model matrices is:

$$[\mu_{sm}^{rom}] = [I] \ , \ [\kappa_{sm}^{rom}] = [\Lambda^s] + \sum_{n=1\ldots N} [q]_n^T \cdot \underset{p=1\ldots P}{diag} \left(\delta_{b,p}^n \cdot \lambda_{b,p}^0\right) \cdot [q]_n ; \tag{17}$$

where the summation in the stiffness matrix equation can be introduced since the blades are not directly coupled together (the matrix $\left[K_b^\delta\right]$ is block diagonal).

3. Integral Mode Mistuning (IMM)

. An alternative reduced-order model, accomplishing for the introduction of the sector frequency mistuning, can be obtained through an extension of the CMM technique ([23]). The key-idea is to change the definition of the second CMM component, i.e. substituting the blade mistuning component with a **sector mistuning component**, as shown in Figure 1(b).

Considering a structural perturbation applied to the whole sector, the matrices $\left[M^\delta\right]$ and $\left[K^\delta\right]$ are no longer block diagonal, since the sectors are directly coupled together; moreover, due to the different perturbation among the sectors, these matrices are not circulant. Let us re-order the displacement dofs of the two components as:

$$\left\{x^s\right\} = \begin{bmatrix} x_r^{S,1} \equiv x_l^{s,n} \\ x_i^{S,1} \\ x_r^{S,2} \equiv x_l^{S,1} \\ x_i^{S,2} \\ \vdots \\ x_r^{s,n} \equiv x_l^{S,N-1} \\ x_i^{s,n} \end{bmatrix}; \qquad \left\{x^\delta\right\} = \begin{bmatrix} x_r^{\delta,1} \equiv x_l^{\delta,N} \\ x_i^{\delta,1} \\ x_r^{\delta,2} \equiv x_l^{\delta,1} \\ x_i^{\delta,2} \\ \vdots \\ x_r^{\delta,N} \equiv x_l^{\delta,N-1} \\ x_i^{\delta,N} \end{bmatrix}; \tag{18}$$

where $n = 1....N$ denotes the sector number and the subscripts i, r and l indicate respectively the internal, right and left interfaces dofs. Consequently, the re-ordered stiffness matrix of the sector mistuning component is:

$$\left[K^{\delta}\right] = \\ = \begin{bmatrix} K_{rr}^{\delta,1} + K_{ll}^{\delta,N} & K_{ri}^{\delta,1} & 0 & 0 & \cdots & 0 & K_{li}^{\delta,N} \\ K_{ir}^{\delta,1} & K_{ii}^{\delta,1} & K_{il}^{\delta,1} & 0 & \cdots & 0 & 0 \\ \vdots & \vdots & \vdots & \ddots & \ddots & \vdots & \vdots \\ \vdots & \vdots & \vdots & \vdots & \ddots & \vdots & \vdots \\ 0 & 0 & 0 & 0 & K_{ri}^{\delta,N-1} & K_{rr}^{\delta,N} + K_{ll}^{\delta,N-1} & K_{ri}^{\delta,N} \\ K_{il}^{\delta,N} & 0 & 0 & 0 & 0 & K_{ir}^{\delta,N} & K_{ii}^{\delta,N} \end{bmatrix}. \tag{19}$$

By using the same approach described in section 2, where $[\Phi_b^s]$ are now replaced by the whole tuned eigenvectors $[\Phi^s]$, the mass and stiffness matrices of the IMM model, with the small mistuning approximation, can be written in place of (11):

$$[{\mu_{sm}}^{rom}] = [I] + \left[\phi^{sT} \cdot M^{\delta} \cdot \phi^{s}\right] \ , \ [{\kappa_{sm}}^{rom}] = [\Lambda^{s}] + \left[\phi^{sT} \cdot K^{\delta} \cdot \phi^{s}\right]. \tag{20}$$

Let us now explicit the bracketed product of the stiffness matrix in (20):

$$\begin{aligned} \left[\phi^{sT} \cdot K^{\delta} \cdot \phi^{s}\right] = \sum_{n=1.....N} \Big(& [\phi_r^{s,n}]^T \cdot \left[K_{rr}^{\delta,n}\right] \cdot [\phi_r^{s,n}] + \\ & + \left[\phi_r^{S,n+1}\right]^T \cdot \left[K_{ll}^{\delta,n}\right] \cdot \left[\phi_r^{S,n+1}\right] + [\phi_i^{s,n}]^T \cdot \left[K_{ir}^{\delta,n}\right] \cdot [\phi_r^{s,n}] + \\ & + [\phi_i^{s,n}]^T \cdot \left[K_{il}^{\delta,n}\right] \cdot \left[\phi_r^{S,n+1}\right] + [\phi_r^{s,n}]^T \cdot \left[K_{ri}^{\delta,n}\right] \cdot [\phi_i^{s,n}] + \\ & + [\phi_i^{s,n}]^T \cdot \left[K_{ii}^{\delta,n}\right] \cdot [\phi_i^{s,n}] + \left[\phi_r^{S,n+1}\right]^T \cdot \left[K_{li}^{\delta,n}\right] \cdot [\phi_i^{s,n}] \Big) \end{aligned} \tag{21}$$

The nth addend can be rewritten as the matrix product:

$$\begin{bmatrix} \phi_r^{s,n} \\ \phi_i^{s,n} \\ \phi_r^{S,n+1} \end{bmatrix}^T \cdot \begin{bmatrix} K_{rr}^{\delta,n} & K_{ri}^{\delta,n} & 0 \\ K_{ir}^{\delta,n} & K_{ii}^{\delta,n} & K_{il}^{\delta,n} \\ 0 & K_{li}^{\delta,n} & K_{ll}^{\delta,n} \end{bmatrix} \cdot \begin{bmatrix} \phi_r^{s,n} \\ \phi_i^{s,n} \\ \phi_r^{S,n+1} \end{bmatrix} = [\phi^{s,n}]^T \cdot \left[K^{\delta,n}\right] \cdot [\phi^{s,n}]\,; \tag{22}$$

i.e., the projection of the nth sector stiffness matrix $\left[K^{\delta,n}\right]$ in the correspondent nth sector portion $[\phi^{s,n}]$, including left and right interfaces dofs, of the tuned modal matrix.

As a consequence, also in this case, it is possible to introduce the summation seen in (17); the great advantage is that the cantilevered blade normal modes used in the classical CMM technique are replaced with the normal modes $[\phi_s^0]$ of the whole basic sector, with its left and right interfaces kept free. The replacement is accomplished, as done for the classical CMM model, by introducing the participation factors $[q]$:

$$\left[\phi_s^0\right]^T \cdot [K_0] \cdot \left[\tilde{\phi}_s^{s,h}\right]_n = \left[\phi_s^0\right]^T \cdot [K_0] \cdot \left[\phi_s^0\right] \cdot \left[\tilde{q}^h\right]_n = [\Lambda_0] \cdot \left[\tilde{q}^h\right]_n, \tag{23}$$

being $[M_0]$ and $[K_0]$ are the mass and stiffness matrices of the unperturbed single sector and $[\Lambda_0]$ contains its eigenvalues, it is possible to express the tuned eigenvectors $\left[\phi_s^{s,h}\right]_n$ as linear combination of the free-interface sector modes $[\phi_s^0]$; substituting the (21) in the (20), without mass mistuning, we obtain:

$$[\mu_{sm}^{rom}] = [I]\,; \tag{24}$$

$$\begin{aligned} [\kappa_{sm}^{rom}] = [\Lambda^s] + \left[\phi^{sT} \cdot K^{\delta} \cdot \phi^s\right] = \\ = [\Lambda^s] + \sum_{i=1....N} [q]_n^T \cdot \left[\phi_s^0\right]^T \cdot \left[K^{\delta,n}\right] \cdot \left[\phi_s^0\right] \cdot [q]_n\,. \end{aligned} \tag{25}$$

Now it is possible to apply the mistuning projection method:

$$\left[\kappa^{\delta}\right]_n = \left[\phi_s^0\right]^T \cdot \left[K^{\delta,n}\right] \cdot \left[\phi_s^0\right] = \underset{p=1...P}{diag}\left(\delta_{s,p}^n \cdot \lambda_p^0\right) \quad \text{with } n = 1...N, \tag{26}$$

where δ_p^n is the nth sector frequency mistuning for mode p, defined as the deviation of the pth natural frequency λ_p^0 of the free-interface sector.

The IMM matrices are, finally:

$$[\mu_{sm}^{rom}] = [I] \ , \ [\kappa_{sm}^{rom}] = [\Lambda^s] + \sum_{i=1....N} [q]_n^T \cdot \underset{p=1...P}{diag} \left(\delta_{s,p}^n \cdot \lambda_r^0\right) \cdot [q]_n \, . \tag{27}$$

We can conclude that, by introducing the free-interface sector modes instead of the single cantilevered blade modes into the CMM formulation, it is possible to obtain an alternative version of this ROM, here referred as IMM, that keeps the high-performing characteristics of the original technique.

4. Numerical validation

. In order to validate the CMM extension proposed in the previous section, a whole finite element model of a real, manufactured dummy bladed disk, consisting of 18 sectors, is chosen as benchmark (Figure 2(c)). In order to better reproduce the real blade-disk interface, a dovetail blade root geometry has been adopted.

The centrifugal force effect is simulated through two screws (Figure 2(b)) pressing the blade root against the slot on the disk rim. Between the screws heads and the blade are provided two washers to uniformly distribute the load. The assembly is designed in order to obtain a stagger angle of the blades equal to 45 degrees. The material used is a C40 hardened and tempered steel.

The benchmark FEM is analysed with the ANSYS software, and consists of 81054 dofs. The disk is constrained at the inner circle radius; in order to simplify the mesh grid, the washers has been uniformly distributed along the slot axial thickness, as shown in Figure 2(c); the washer volumes are completely fixed to both the blades and the disk. On the contrary, only a couple of nodes for each side of the disk-slots and blade-roots are forced to experience the same displacement, as highlighted by the green constraints displayed in Figure 2(c).

The modal analysis of the tuned model produces the natural frequencies over nodal diameter diagram shown in Figure 2(d): only the frequency band including the first modal family is taken into account. The forced response is calculated by applying a rotating force, defined in (2), whose amplitude

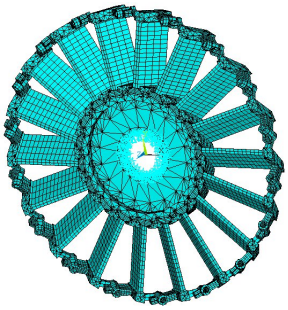

(a) Whole FE model.

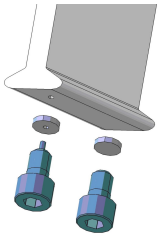

(b) Blade-disk assembly.

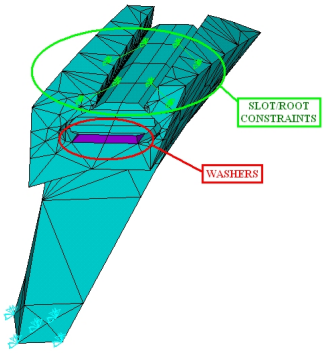

(c) Blade-disk coupling.

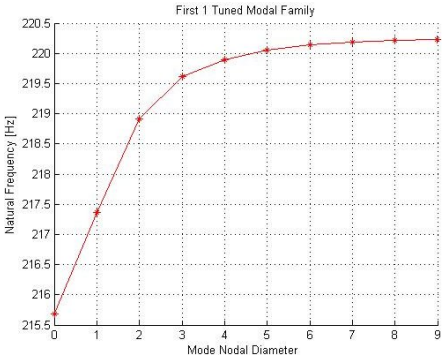

(d) First family of modes for the tuned bladed disk chosen.

Figure 2: The FEM test-case chosen as benchmark for the IMM validation process.

is 10 N, applied along the axial direction to a node at the tip of each blade; a constant modal damping $\zeta = 0.001$ is introduced both in the FE and RO models, so that the modal damping matrix elements are:

$$[\phi_i]^T \cdot [C] \cdot [\phi_i] = 2 \cdot \zeta \cdot \omega_i; \tag{28}$$

where $[\phi_i]$ is the ith eigenvector and ω_i is the correspondent squared root eigenvalue, $\omega_i = 2\pi f_i$. As a consequence, when a mistuning pattern is introduced into the structure, also the damping matrix is perturbed due to the occurred frequency change.

Two mistuning patterns are introduced on the tuned finite element model: (i) a blade frequency mistuning pattern, consisting of deviations in the blades

Sector	**(a)** $\delta_E^{(b)}$	**(b) Roots**	**Sector**	**(a)** $\delta_E^{(b)}$	**(b) Roots**
1	0.0059	all	*10*	-0.0207	all
2	-0.0169	front	*11*	0.0045	back
3	0.0083	front	*12*	-0.0166	front
4	-0.0049	back	*13*	0.0012	front
5	-0.0077	all	*14*	-0.0157	back
6	-0.0053	back	*15*	-0.0030	all
7	-0.0016	back	*16*	-0.0218	back
8	0.0057	front	*17*	-0.0003	all
9	0.0142	all	*18*	-0.0116	all

Table 1: Mistuning patterns introduced in the FE model: (a) blade elastic modulus deviations (mean = -0.005, st.dev. = 0.01), (b) blade-to-disk mistuning: the side of the coupled nodes is indicated.

elastic modulus (numerically generated from a normal distribution with zero mean and 1% standard deviation), and (ii) a sector-to-blade interfaces mistuning, by changing the root/slot coupling. In the former case, the mistuning pattern is selected, through a Monte Carlo analysis consisting of 5000 iterations (performed by using a reduced CMM model of the bladed disk), as the pattern which produces the maximum forced response amplification for an EO 9 excitation; in the latter case, the idea is to reproduce a typical mistuning pattern coming out from the assembly of the whole structure: in this case, the mistuning is due to a different tightening of the two screws used to reproduce the centrifugal force effect. This condition has been modelled in the FEM by uncoupling the front or back couples of nodes shown in Figure 2(c). The two mistuning patterns are listed in Table 1.

The reduced-order model is generated including the first 18 tuned modes shapes $[\Phi^s]$: then, its final dimension is equal to 18 dofs, corresponding to the 0.022% of the whole finite element model. Moreover, in order to apply the mistuning projection method, the first 20 free-interface single sector normal modes $[\Phi_s^0]$ are retained. The proposed IMM technique is employed in order to obtain the reduced-order model (ROM) of the whole structure. As explained in the previous section, it is suitable for the introduction of a *sector frequency mistuning* pattern; there is so the need to identify the "real" mistuning (root/slot coupling + blade Young modulus deviations) of the structure as deviations of the fundamental sector frequencies (δ_s^n). This

goal is achieved by providing a numerical one-to-one relation between the two different mistuning patterns, i.e. using a proper FE model to calculate, sector by sector, the frequency deviations caused by the real mistuning. For this purpose, a tuned FE model of the whole structure is chosen where, one-by-one, the different mistuning values of Table 1 are applied equally to each sector; then, the consequent median nodal diameter (the fourth in this case) frequency deviation is taken as representative of the sector frequency deviation. This approach is based on the considerations proposed by Griffin et al. in [18]: if the modal family of interest is sufficiently isolated (as the one of Figure 2(d)) from the others, all the modes of this family can be represented by means of the same basis of the fundamental sector modes: consequently, the tuned median nodal diameter frequency deviation is representative of the single sector frequency deviations. By using the same numerical relation described above, we can also evaluate that the root/slot mistuning pattern (considered alone) has a mean, in terms of sector elastic modulus deviation, equal to -0.007 and a standard deviation equal to 0.6%: consequently, the root/slot and blade mistuning patterns considered in our analysis are comparable.

The sector frequency mistuning pattern δ_s^n is then introduced into the ROM (see equation (27)); the comparison between the ROM prediction and the FEM benchmark concerns:

1. Mistuned natural frequencies;
2. Mistuned mode shapes, through the Modal Assurance Criterion (MAC);
3. Maximum forced responses of the whole blisk to some EO excitations.

In order to investigate the ROM accuracy in predicting the mistuned frequencies, the percentage error defined by the (29) is commonly found in literature:

$$\varepsilon = \left| \frac{f_{rom}^{(mist)} - f_{fem}^{(mist)}}{f_{fem}^{(mist)}} \right| \cdot 100, \tag{29}$$

where f denotes a natural frequency. However, this error index does not give a full view about the real quality of the prediction, because the ROM has to be able also to capture the frequency split due to mistuning. This means that the ROM mistuned frequencies have to be, not only close to the FEM ones, but *closer to the FEM ones than to the tuned ones*. A frequency split percentage error must be defined to complete the information given

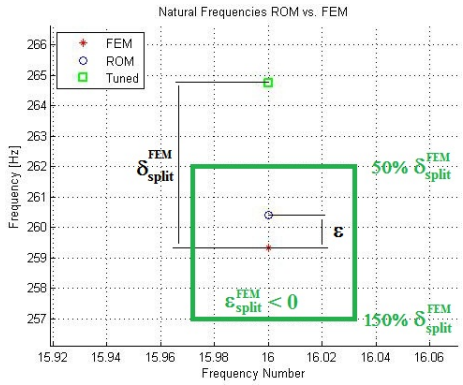

Figure 3: Definition of the error $\varepsilon_{split}^{FEM}$ in capturing the frequency splits.

by the error (29). By defining the "real" frequency split obtained by FEM calculation as:

$$\Delta_{split}^{FEM} = \frac{f_{fem}^{(mist)} - f_{tuned}}{f_{tuned}} \cdot 100, \tag{30}$$

we suggest to adopt the following frequency split error:

$$\varepsilon_{split}^{FEM} = \varepsilon - \left| \Delta_{split}^{FEM} / 2 \right|. \tag{31}$$

To understand the meaning of the (31), look at the example shown in Figure 3: we can assume that the frequency split is captured if the ROM mistuned frequency lies within the up and bottom sides of the green square, i.e., if it is closer to the FEM frequency than to the tuned one. In this case, the error $\varepsilon_{split}^{FEM}$ is less than zero, denoting a clear threshold under which the frequency split can be considered as captured by the ROM. Note that when the split δ_{split}^{FEM} approaches zero, the error $\varepsilon_{split}^{FEM}$ tends to the error ε.

The results of the validation process are shown in Figure 4. As expected, the accuracy of the IMM model is quite close to that obtained from the original CMM model in [21]: the average error ε in the mistuned frequencies estimation, plotted in Figure 4(b), is 0.05%. Note that the greater error occurring for the lower frequencies is due to the accuracy involved in the mistuning identification, since the median nodal diameter frequency, used as representation of the the sector frequency mistuning, is included in the

high modal density region (nodal diameters greater than 3 in Figure 2(d)); as a consequence, the mistuned frequencies of the blade-dominated modes are excellently modelled. The slight inaccuracy of the identified mistuning pattern influences also the mode shapes calculation: the minimum MAC (Figure 4(d)) is 0.61 for the eleventh mode, with a mean of 0.91; moreover, Figure 4(c) shows that the frequency split is optimally captured. The results shown for the modal analysis are confirmed also by the forced response calculation: as an example, the maximum forced response amplification, for an EO 9 excitation (Figure 4(e)), computed by the ROM is 66.32% higher than the tuned response, against the 66.34% computed by the FEM.

The validation process described above confirms that a sector mistuning model is suitable to correctly capture both the blade and slot/root mistuning. On the other hand, the necessity to adopt a sector mistuning model instead of a simple blade mistuning model to accurately predict the whole structure dynamics is not evident; we need to verify that the slot/root mistuning is not negligible with respect to the blade frequency mistuning. This validation is accomplished by the generation of a further ROM, through the original CMM technique, where only the blade elastic modulus deviations of Table 1 are introduced. The results are displayed in Figure 5. It is evident that a blade frequency mistuning model is not enough for the case of interest; moreover, if we calculate the maximum resonant forced response amplifications, listed in Table 2, obtained both from the CMM and IMM models for some EO excitation, it is possible to see how much the mistuning applied to the disk-to-sector interface can sensibly, and sometimes negatively, influence the structure dynamics. See, for instance, the 12% higher amplification obtained by the IMM ROM with respect to the CMM model for EO 8 excitation.

Engine Order excitation	**Amplifications** [%]		
	FEM	**IMM**	**CMM**
6	20	21	30
7	**34**	37	32
8	**53**	53	41
9	66	66	73

Table 2: Maximum forced response amplifications, with respect to the tuned bladed disk, computed by the ROMs.

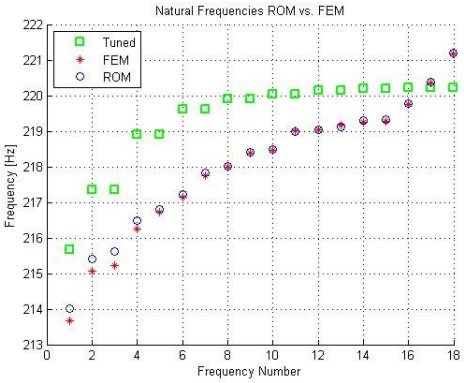

(a) Mistuned natural frequencies.

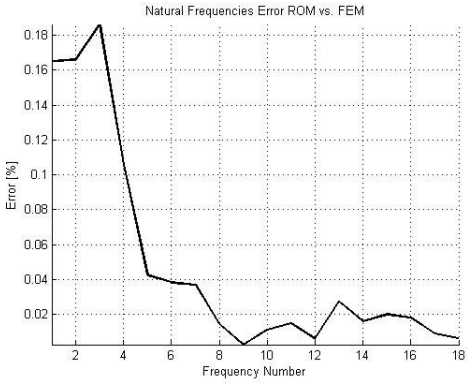

(b) Mistuned natural frequencies error ε.

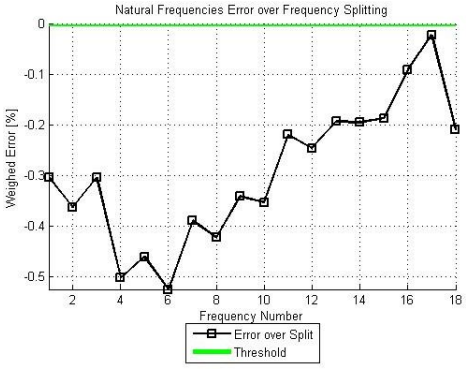

(c) Mistuned natural frequencies error over frequency split $\varepsilon_{split}^{FEM}$.

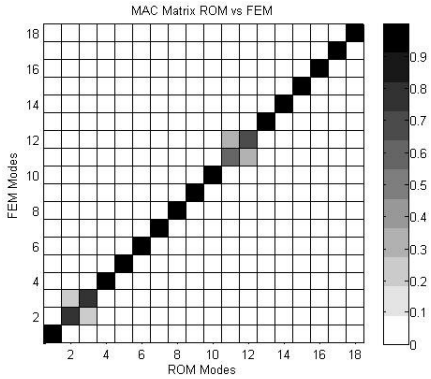

(d) Mistuned mode shapes MAC.

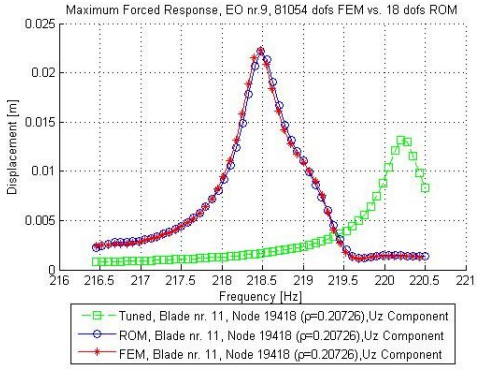

(e) Maximum forced response tuned vs. mistuned to E.O. 9 excitation.

Figure 4: Comparison between IMM ROM and FEM results.

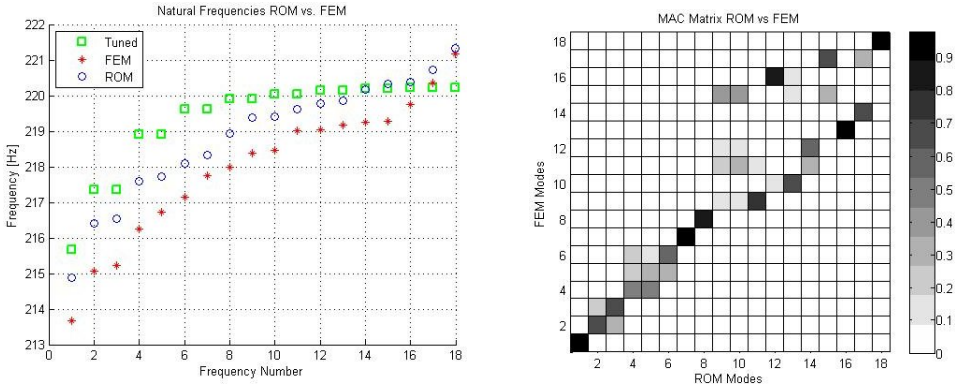

(a) Mistuned natural frequencies.

(b) Mistuned mode shapes MAC.

Figure 5: Comparison between CMM ROM and FEM results.

5. Conclusion

In this paper, a pre-existing high-performing order reduction technique for finite element models, the so-called CMM, is extended to allow for the introduction of a sector frequency mistuning pattern. This extension is referred as Integral Mode Mistuning (IMM) model. In order to validate such technique, the FE model of a real, manufactured dummy bladed disk is chosen as benchmark. Two mistuning patterns are superimposed in the tuned structure: (i) a classical blade frequency mistuning, introduced as deviations of the single blades elastic modulus, and (ii) a disk-to-blade interface mistuning, as slight slot/root constraint modifications. Three tasks are chosen for the validation process:

1. To investigate the quality of the IMM predictions, as already assessed for the CMM model, by means of the comparison of the following modal quantities between the ROM and the benchmark FEM: mistuned natural frequencies, mode shapes and forced responses.
2. To verify that a sector mistuning model can be more suitable than a blade mistuning model to correctly predict the whole structure dynamics.
3. To show how the addition of the slot/root mistuning can lead to higher forced response amplitudes than those provided by the blade mistuning only.

All the goals listed above are reached: the highly reduced-order model obtained with the IMM technique shows an excellent accuracy, both for the modal parameters (natural frequencies and mode shapes) and forced response predictions; moreover, if the blade mistuning only is applied to the ROM, the whole structure dynamics may be not well captured; finally, a higher maximum forced response may occur if the slot/root mistuning is added to the blade mistuning.

References

[1] Ewins, D.J., The Effects of Detuning upon the Vibrations of Bladed Disks, Ph.D. Thesis, University of Cambridge, 1966.

[2] Mead, D.J., A General Theory of Harmonic Wave Propagation in Linear Periodic Systems with Multiple Coupling, Journal of Sound and Vibration, Vol. 27, No. 2, 1973, pp. 235-260.

[3] Thomas, D.L., Dynamics of Rotationally Periodic Structures, International Journal for Numerical Methods in Engineering, Vol. 14, 1979, pp. 81-102.

[4] Hodges, C.H., Confinement of Vibration by Structural Irregularity, Journal of Sound and Vibration, Vol. 82, No. 3, 1982, pp. 411-424.

[5] Hodges, C.H. and Woodhouse, J., Vibration isolation from Irregularities in a Nearly-Periodic Structure: Theory and Measurements, Journal of Acoustical Society of America, Vol. 74, No. 3, 1983, pp. 894-905.

[6] Griffin, J.H., and Hoosac, T.M., Model Development and Statistical Investigation of Turbine Blade Mistuning, Journal of Vibration, Acoustics, Stress and Reliability in Design, Vol. 106, 1984, pp.204-210.

[7] MacBain, J.C., and Whaley, P.W., Maximum Resonant Response of Mistuned Bladed Disks, Journal of Vibration, Acoustics, Stress and Reliability in Design, Vol. 106, 1984, pp. 218-223.

[8] Kissel, G.J., Localization in Disordered Periodic Structures, Ph.D. Thesis, Massachusetts Institute of Technology, 1988.

[9] Pierre, C., Mode Localization and Eigenvalue Loci Veering Phenomena in Disordered Structures, Journal of Sound and Vibration, Vol. 126, No. 3, 1988, pp. 485-502.

[10] Óttarson, G.S. and Pierre, C., A Transfer Matrix Approach to Free Vibration Localization in Mistuned Blade Assemblies, Journal of Sound and Vibration, Vol. 197, No. 5, 1996, pp. 589-618.

[11] Castanier, M.P., ttarson, G.S. and Pierre, C., A Reduced Order Modeling Technique for Mistuned Bladed Disks, Journal of Vibration and Acoustics, Vol. 119, 1997, No. 3, pp. 439-447.

[12] Yang, M.-T., and Griffin, J.H., A Normalized Modal Eigenvalue Approach for Resolving Modal Interaction, Journal of Engineering for Gas Turbines and Power, Vol. 119, 1997, pp. 647-650.

[13] Whitehead, D.S., The Maximum Factor by Which Forced Vibration of Blades Can Increase Due to Mistuning, Journal of Engineering for Gas Turbines and Power, Vol. 120, 1998, pp. 115-119.

[14] Bladh, R., Castanier, M.P. and Pierre, C., Reduced Order Modeling and Vibration Analysis of Mistuned Bladed Disk Assemblies with Shrouds, Proceedings of the 43rd ASME Gas Turbine and Aeroengine Technical Congress, Exposition and Users Symposium, Stockholm, Sweden, June 1998.

[15] Yang, M.-T., and Griffin, J.H., A Reduced-Order Model of Mistuning Using a Subset of Nominal System Modes, Journal of Engineering for Gas Turbines and Power, Vol. 123, 2001, pp. 893-900.

[16] Feiner, D.M., and Griffin, J.H., A Fundamental Model of Mistuning for a Single Family of Modes, Journal of Turbomachinery, Vol.124, 2002, pp. 597-605.

[17] Petrov, E.P., Sanliturk, K.Y., and Ewins, D.J., A New Method for Dynamic Analysis of Mistuned Bladed Disks Based on the Exact Relationship Between Tuned and Mistuned Systems, Journal of Engineering for Gas Turbines and Power, Vol. 124, No. 3, 2002, pp. 586-597.

[18] Feiner, D.M. and Griffin, J.H. Mistuning Identification of Bladed Disks Using a Fundamental Mistuning Model - Part I: Theory, Journal of Turbomachinery, Vol. 126, 2004, pp. 150-158.

[19] Feiner, D.M. and Griffin, J.H. Mistuning Identification of Bladed Disks Using a Fundamental Mistuning Model - Part II: Application, Journal of Turbomachinery, Vol. 126, 2004, pp. 159-165.

[20] Castanier, M.P., Pierre, C., Modeling and Analysis of Mistuned Bladed Disk Vibration: Status and Emerging Directions, Journal of Propulsion and Power, Vol. 22, No. 2, 2006, pp. 384-396.

[21] Lim, S.-H., Bladh, R., Pierre, C., and Castanier, M.P., Compact, Generalized Component Mode Mistuning Representation for Modeling Bladed Disk Vibration, AIAA Journal, Vol. 45, No. 9, 2007, pp. 2285-2298.

[22] Avalos, J., Mignolet, M.P., and Soize, C., Response of Bladed Disks With Mistuned Blade-Disk Interfaces, Proceedings of the 2009 ASME Turbo Expo, Orlando, Florida, USA, June 2009.

[23] Vargiu, P., Analysis of mistuned bladed disk vibrations on aircraft jet engines, Ph.D. Thesis, Politecnico di Torino, 2010.